JTTEES 7:546-552

The Effect of Residual Stress in HVOF Tungsten Carbide Coatings on the Fatigue Life in Bending of Thermal Spray Coated Aluminum

R.T.R. McGrann, D.J. Greving, J.R. Shadley, E.F. Rybicki, B.E. Bodger, and D.A. Somerville

(Submitted 16 January 1998; in revised form 22 May 1998)

One factor that affects the suitability of tungsten carbide (WC) coatings for wear and corrosion control applications is the fatigue life of the coated part. Coatings, whether anodized or thermal spray coated, can reduce the fatigue life of a part compared to an uncoated part. This study compares the fatigue life of uncoated and thermal spray coated 6061 Al specimens. The relation between the residual stress level in the coating and the fatigue life of the specimen is investigated.

Cyclic bending tests were performed on flat, cantilever beam specimens. Applied loads placed the coating in tension. Residual stress levels for each of the coating types were determined experimentally using the modified layer removal method.

Test results show that the fatigue life of WC coated specimens is directly related to the level of compressive residual stress in the coating. In some cases, the fatigue life can be increased by a factor of 35 by increasing the compressive residual stress in the coating.

Keywords coating-WC-Co, fatigue, HVOF, residual stress, substrate-6061Al

1. Introduction

Wear and corrosion control of many aircraft components is currently accomplished by chrome plating or hard anodizing. However, problems associated with these operations are compelling the aircraft industry to search for alternative processes. One problem is that anodizing is not an adequate solution for control of wear and corrosion of parts in some situations.

Tungsten carbide (WC) coating applied by the high velocity oxy-fuel (HVOF) process is a candidate for replacing anodizing. Aircraft manufacturers are investigating this coating for use on helicopter components. High velocity oxy-fuel WC coating is being examined in different types of tests, including fatigue. The focus of the investigation described in this paper is to evaluate the bending fatigue life of HVOF tungsten carbide coated aluminum specimens.

Various coating systems that give improved wear properties may cause a drastic reduction in the fatigue life of a component due to cracking that starts in the coating and penetrates into the substrate material. The result can be cracks propagating through the substrate, resulting in loss of function of the component. Chrome plating and anodizing create such a reduction in fatigue life. Experiments have shown that chrome plated parts, while producing improved wear properties, have fatigue lives that are shorter than those of uncoated parts (Ref 1). This reduction is called a fatigue deficit. To alleviate the fatigue deficit, parts are made thicker to reduce in-service stresses and thereby restore the fatigue life to levels that would be near those for the uncoated part. Designing for a fatigue deficit, whether due to chrome plating or anodizing, costs money because of the heavier construction required and because heavier aircraft parts reduce payload and increase fuel consumption.

It is also known that fatigue crack initiation is a surface phenomenon related to the residual stress level near the surface (Ref 2). Compressive residual stresses can increase the number of cycles before crack initiation begins through a mean stress effect (Ref 3). Due to the high temperatures associated with most thermal spray processes and differences in coefficients of thermal expansion between the coating and the substrate materials, residual stresses in the coating are unavoidable. Therefore, it is important to know the relation between residual stress levels in the coating and the fatigue life of the thermal spray coated part.

In the following sections, the objectives and approach used to determine the relation between coating residual stress levels and fatigue life are described. A description of the testing program that was followed to evaluate the fatigue life of HVOF tungsten carbide coatings on aluminum is given. The results of the investigation are presented, as well as a summary and conclusions.

2. Objectives

The work described here is part of a larger project with the overall goal of using the wear characteristics, environmentally

R.T.R. McGrann, D.J. Greving, J.R. Shadley, and **E.F. Rybicki,** Department of Mechanical Engineering, The University of Tulsa, Tulsa, OK 74104, USA. Contact e-mail: mcgrann@binghamton.edu. D.J. Greving is presently with AlliedSignal Engines, Phoenix, AZ, USA. **B.E. Bodger and D.A. Somerville,** Southwest Aeroservice, Inc., Tulsa, OK, 74120, USA. B.E. Bodger is presently with Sulzer Metco (US) Inc., Westbury, NY, USA. R.T.R. McGrann is presently with State University of New York, Binghamton, NY 13905-6000, USA.

friendly qualities, and other advantages of WC thermal spray coatings to identify applications where WC coatings can replace hard chrome plating or anodizing. Requirements to achieve this overall goal include gaining an understanding of the response of WC coatings for different loading conditions and the development of appropriate procedures for applying WC coatings.

Many potential replacement applications of WC coatings involve cyclic loadings that require high fatigue resistance of the WC coating. It is well known that surface residual stresses play an important role in resistance to fatigue damage. The primary goal of this work is to determine the effect of coating residual stresses on the fatigue life of WC coated parts. Because coating residual stresses are controlled by the coating process application parameters, the results of this work indicate factors to be considered in the design of coatings and the selection of coating application process parameters.

3. Approach

The approach to accomplishing the objective of this work was, first, to select a coating type and substrate material. An 83%WC-17%Co coating was selected. Since many potential anodizing replacement applications are for aircraft, a substrate material commonly used in aircraft construction was selected. The substrate material chosen was 6061-T6511 Al.

To simulate in-service loads and to supplement existing axial fatigue test data, a bending fatigue test was chosen. Processing parameters for HVOF were selected to produce three sets of specimens with a different level of residual stress in the coating for each set. Specimens for residual stress evaluation and specimens for fatigue testing were processed together.

The through-thickness residual stress distribution in each specimen was determined using the modified layer removal method (MLRM, Ref 4). An average residual stress in the coating for each of the three residual stress levels was calculated. Bending fatigue tests were conducted at three maximum deflections. Fatigue life curves (*S-N* curves) were developed for each of the three levels of average residual stress in the coating.

4. Experimental Procedure

Description of the experimental procedure is presented in four subsections: (1) Residual Stress and Fatigue Specimen Description, (2) Procedure for Evaluating Residual Stresses, (3) Fatigue Testing, and (4) Test Matrix.

4.1 Residual Stress and Fatigue Specimen Description

The typical dimensions and materials of the residual stress specimens are shown in Fig. 1. Square specimens, 25.4 mm by 25.4 mm (1 in. × 1 in.), were prepared. The typical substrate thickness was 3.18 mm (0.125 in.). The material properties used for the coating were experimentally determined using the cantilever beam bending method (CBBM Ref 5). For the WC coating, the material properties are a Young's modulus (E_c) of 179.6 GPa (26 Msi) and a Poisson's ratio of (ν_c) of 0.27. For the aluminum substrate, a Young's modulus (E_s) of 70 GPa (10 Msi) and a Poisson's ratio (ν_s) of 0.33 were used (Ref 6). These are the values that are used in the calculation of the residual stresses. Other studies have shown that the Young's modulus of the coating can vary with the application procedure (Ref 7), the method used in this study to determine the residual stress in the coating is not especially sensitive to the value used for the coating modulus (Ref 8). For reference, the yield stress of 6061-T65 is 276 MPa (40 ksi), the ultimate stress is 310 MPa (45 ksi), and the rotating-bending fatigue limit is 97 MPa (14 ksi, Ref 9).

Surfaces were polished prior to coating. Hand polishing was performed with a polishing cloth until a mirror finish was achieved. Edges were beveled by hand polishing. No shot peening or grit blasting was used. The specimens were coated using Jet Kote II HVOF spray equipment (Stellite Coatings, Goshen, IN). The final coating thickness was 0.17 mm (6.5 mils). After coating, the specimen sides were polished to remove any overspray.

The fatigue specimen used was a tapered, cantilever beam specimen. Typical dimensions of the specimen are shown in Fig. 2. Preparation of the fatigue specimens was performed in exactly the same manner as the residual stress specimens. The surface area that is coated, between the radius at each end, is tapered to give an area of constant bending stress along the coated length. Specimens were designed to fail in this region when the small end was loaded with a downward bending load, putting the coated side in tension.

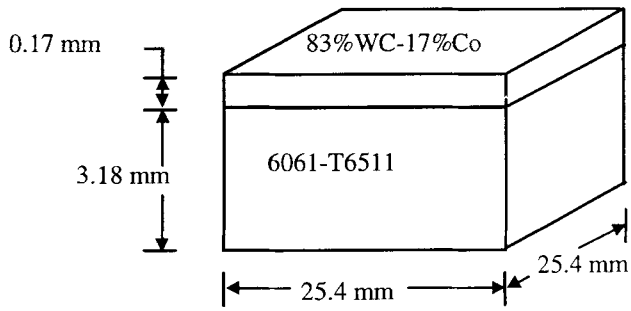

Fig. 1 Residual stress specimen dimensions and materials

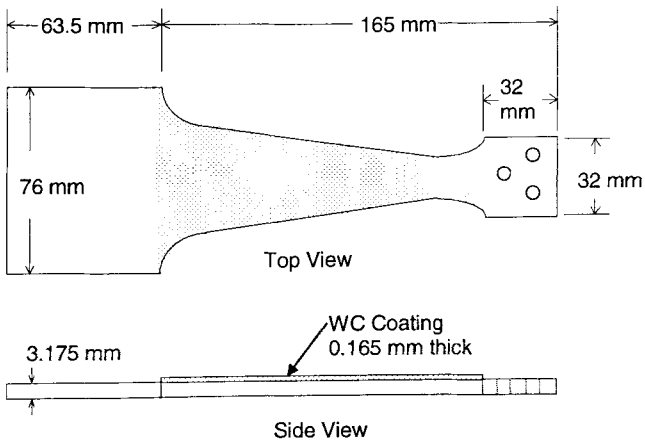

Fig. 2 Typical dimensions of bending fatigue specimen

4.2 Procedure for Evaluating Residual Stresses

The MLRM (Ref 4) was used to determine the through-thickness residual stress distributions in the coating. The procedure involves attaching strain gauges to the uncoated side of the residual stress specimen and removing thin layers of the coating. Layers of about 0.05 mm (2 mils) are removed from the coating by polishing using a metallurgical polishing wheel. Thickness measurements of the specimen are made after each layer is removed.

Changes in strain gauge readings are recorded as layers are removed. The strain and thickness changes are inputs for the residual stress analysis back-computation procedure. The analysis is applied to each layer removed and calculates the residual stress in the layer removed and the change in stress distribution for the remaining piece. The stresses are summed in the back-computation procedure, for each layer removed, to evaluate the residual stress distribution in the material removed. The stress distribution that was originally in the material is computed from the stresses in the material removed.

4.3 Fatigue Testing

The tapered beam fatigue specimens were loaded in a cantilever bending fixture using the Fatigue Dynamics, Inc. (Walled Lake, MI) adjustable bending machine shown in Fig. 3. The small end of the specimen was loaded with an eccentric crank arm that applied a repeated maximum displacement while the large end of the specimen was clamped in a vise. The loading was applied so that the top (coated) surface of the specimen was always in tension. The fatigue loading ranged from a minimum stress that was slightly tensile to a maximum tensile stress, for a minimum/maximum stress ratio, R, of about 0.01.

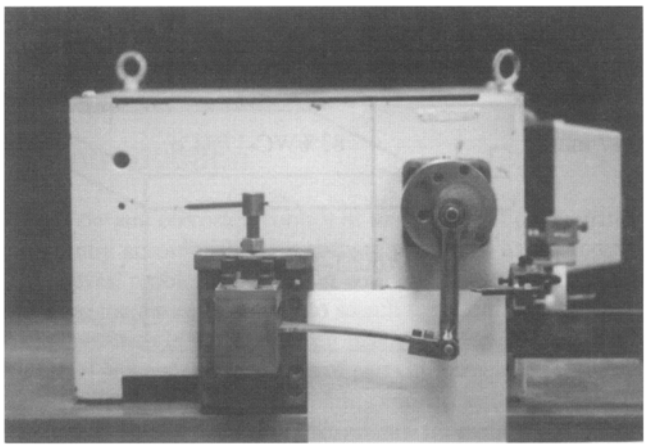

Fig. 3 Bending fatigue test machine

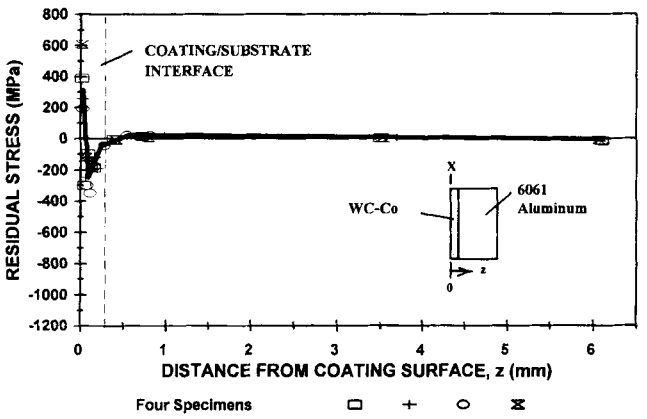

Fig. 4 Through-thickness residual stress distribution for HVOF-WC coated specimens, Spray-1 condition (near neutral coating residual stress)

When the eccentric crank arm is at the top of its stroke, the stress on the specimen top (coated) side is at a minimum. When the eccentric arm is at the bottom of its stroke, as shown in Fig. 3, the stress on the top side is at a maximum tensile value. Longitudinal and transverse maximum and minimum strain values are determined by manually rotating the crank arm to its maximum and minimum deflection points. The maximum and minimum strain values are recorded from biaxial strain gauges attached to the top (coated) surface and to the bottom (substrate). The magnitude of the strain can be controlled by the position of the vise and the amount of stroke that the eccentric crank applies.

The stress at the interface between the coating and the substrate is determined from the strain that is recorded from the strain gauge attached to the bottom of the specimen, on the substrate. An analysis based on the bending of a beam made of two materials (using an equivalent section determined from the ratio of the two Young's moduli) is used to calculate the stress in the substrate at the coating/substrate interface (Ref 10).

The maximum deflection is set using the recorded strain values and held constant throughout the test. The motor to the crankshaft is started, applying the cyclic load at 2000 cpm. Tests were conducted at room temperature. The test was visually monitored until cracking in the coating was suspected. Then, the test was temporarily stopped and a fluorescent dye penetrant test of the specimen was conducted. This test reveals cracks that start at the free surface of the coating. Cracks that begin at the interface are not detectable using this procedure until they propagate to the free surface.

If cracks were indicated, the number of cycles shown on the digital cycle counter was recorded as the number of cycles to crack initiation. Then the test was resumed and continued until the crack propagated through the substrate or runout occurred. If cracks were not detected, periodic stops to check for cracks were continued. When the crack had penetrated through the substrate, the limit switch on the machine turned off the motor and the cycle counter recorded the number of cycles to failure. Failure was defined as separation of the specimen into two pieces. Fatigue testing was terminated (runout occurred) at 10^7 cycles if the specimen had not yet failed.

4.4 Test Matrix

The fatigue and residual stress specimens were prepared so that three different levels of residual stresses were created in the coatings. These sets were designated as Spray-1, Spray-2, and Spray-3. Table 1 shows the test matrix for the residual stress specimens used in this work. A set of uncoated aluminum substrate specimens was also tested.

There are at least 32 variables involved in the coating application using the HVOF spray process. These include powder type, gases used, spray gun operating procedures, and

temperature controls during spraying. The exact parameters of the HVOF process that were varied to create the three levels of coating residual stress in this research are proprietary. However, a few of the variables that were adjusted are shown in Table 2.

The number of fatigue specimens that were sprayed at the same time as the residual stress specimens to create each of the three residual stress levels in the coatings is also shown in Table 1. Fatigue testing was conducted at three deflections for each set of specimens. The typical maximum applied stress levels corresponding to these deflections are shown in Table 3 for two locations in the specimen: (1) in the coating, at the free surface of the coating and (2) in the substrate, at the coating/substrate interface.

5. Results and Discussion

The results of these tests are presented in the following subsections: (1) Through-Thickness Residual Stress Distributions, (2) Average Coating Residual Stress Levels, (3) Fatigue Cycles To Crack Initiation, (4) Fatigue Cycles To Failure, and (5) Trend of Average Coating Residual Stress Level and Fatigue Life.

5.1 Through-Thickness Residual Stress Distributions

The through-thickness residual stress distribution for each of the 16 individual residual stress specimens was determined using the MLRM. The residual stress distributions for the four specimens in the same set are plotted in one figure. Figure 4 shows the through-thickness residual stress distribution for the four specimens of the Spray-1 set, Fig. 5 shows the Spray-2 distribution, and Fig. 6 shows the Spray-3 distribution.

Table 1 Test matrix

	Specimens		Coating compressive residual stress
	Fatigue	Residual stress	
Spray-1	5	4	Near neutral
Spray-2	5	4	Medium
Spray-3	5	4	High
Substrate only	6	4	(None)

Table 2 Selected high velocity oxy-fuel spray parameters

	Spray parameters			
Spray-	H_2 pressure	O_2 pressure	Nozzle length	Nozzle diam
1	Low	Low	Short	Small
2	High	High	Long	Small
3	Medium	Medium	Long	Large

Table 3 Fatigue test matrix

	Maximum applied stress MPa (ksi)				
	Coating at	Substrate at	Number of fatigue specimens		
Deflection	surface	interface	Spray-1	Spray-2	Spray-3
High	450 (65)	190 (28)	1	1	1
Medium	324 (47)	145 (21)	1	3	3
Low	256 (37)	110 (16)	3	1	1

The Spray-1 through-thickness residual stress distribution presented in Fig. 4 shows a surface tensile residual stress of roughly 300 MPa (44 ksi). In a short distance into the coating, approximately 0.04 mm (0.0016 in.), the stress becomes compressive, finally reaching 300 MPa (44 ksi) compressive, and returns to just slightly compressive at the coating/substrate interface.

The Spray-2 condition in Fig. 5 shows a free surface compressive residual stress near 200 MPa (29 ksi) which becomes more compressive as distance into the depth of the coating increases. A maximum compressive residual stress of 800 MPa (116 ksi) is reached. After the peak compressive residual stress was reached, the residual stress becomes less compressive toward the coating/substrate interface. The compressive residual stress level at the interface is approximately 300 MPa (44 ksi).

Figure 6 shows the Spray-3 through-thickness residual stress distribution. This distribution is highly compressive at the free surface, 500 MPa (72 ksi). The distribution becomes more compressive deeper into the coating from the free surface, reaching a maximum compressive residual stress of 1000 MPa (145 ksi). The residual stress is close to 400 MPa (58 ksi) compressive at the coating/substrate interface.

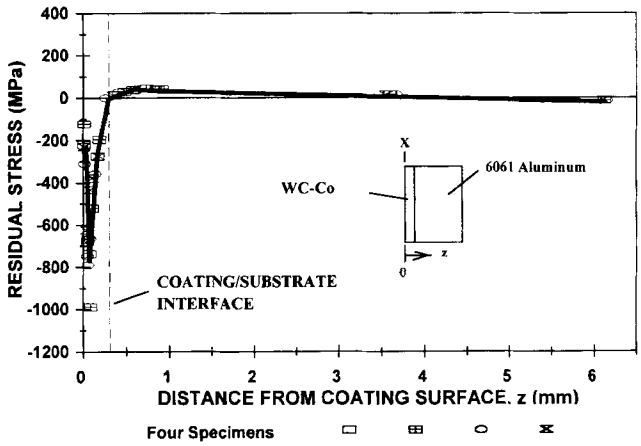

Fig. 5 Through-thickness residual stress distribution for HVOF-tungsten carbide coated specimens, Spray-2 condition (medium coating compressive residual stress)

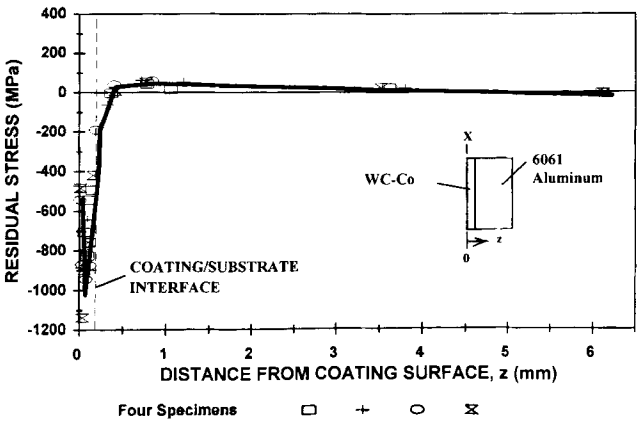

Fig. 6 Through-thickness residual stress distribution for HVOF-tungsten carbide coated specimens, Spray-3 condition (high coating compressive residual stress)

5.2 Average Coating Residual Stress Levels

The average residual stress in the coating was calculated for each set of specimens using the equation:

$$\bar{\sigma} = \frac{\Sigma \sigma \, \Delta t}{\Sigma \, \Delta t}$$

where σ is the stress in a layer removed calculated by the MLRM and Δt is the thickness of the coating layer removed. The average residual stress for each set of specimens and the 95% confidence interval is shown in Table 4.

The expected average residual stress levels were achieved. The Spray-1 set, which was expected to be near neutral, had the lowest average compressive residual stress of approximately 80 MPa (12 ksi). The average residual stress in the coating for the medium compressive set, Spray-2, was above 500 MPa (73 ksi) compressive, and the high compressive set, Spray-3, reached an average residual stress of 760 MPa (110 ksi) compressive.

5.3 Fatigue Cycles To Crack Initiation

The number of cycles to crack initiation (N_i) is shown in Fig. 7 as a function of maximum applied stress. The maximum applied stress is the maximum tensile stress in the substrate at the coating/substrate interface.

This *S-N* curve (stress versus number of cycles) shows the positive effect of increased average compressive residual stress in the coating. The number of cycles to crack initiation at all applied stress levels investigated was higher for the specimens with an average coating compressive residual stress of 500 MPa than for the specimens with an average coating residual stress 80 MPa compressive. Similar fatigue behavior can be seen in Fig. 7 for the specimens with an average coating compressive residual stress of 760 MPa compared to the specimens with 500 MPa coating compressive residual stress. As an example, at a maximum applied stress of 145 MPa, coatings with an average coating compressive residual stress of 80 MPa cracked at around 2.5×10^4 cycles. Coatings with an average compressive residual stress of 500 MPa cracked near 8.0×10^5 cycles and coatings with the highest compressive residual stress of 760 MPa cracked at 3.3×10^6 cycles.

5.4 Fatigue Cycles To Failure

The number of cycles to failure (N_f) versus the maximum applied stress in the substrate at the coating/substrate interface for the coated specimens and the maximum applied stress at the surface of the uncoated substrate specimens is shown in Fig. 8. As with cycles to crack initiation, increased compressive residual stress in the coating increased the life of the specimen. At a maximum applied stress in the coating of 145 MPa, specimens with a compressive residual stress of 80 MPa failed at around 9×10^4 cycles. Specimens with a compressive residual stress of

Table 4 Average compressive residual stress in the coating (95% confidence interval shown)

Designation	Average compressive residual stress, MPa (ksi)
Spray-1	79.7 (11.6) ± 3.3 (0.5)
Spray-2	504.6 (73.2) ± 65.7 (9.5)
Spray-3	761.6 (110.5) ± 118.8 (17.2)

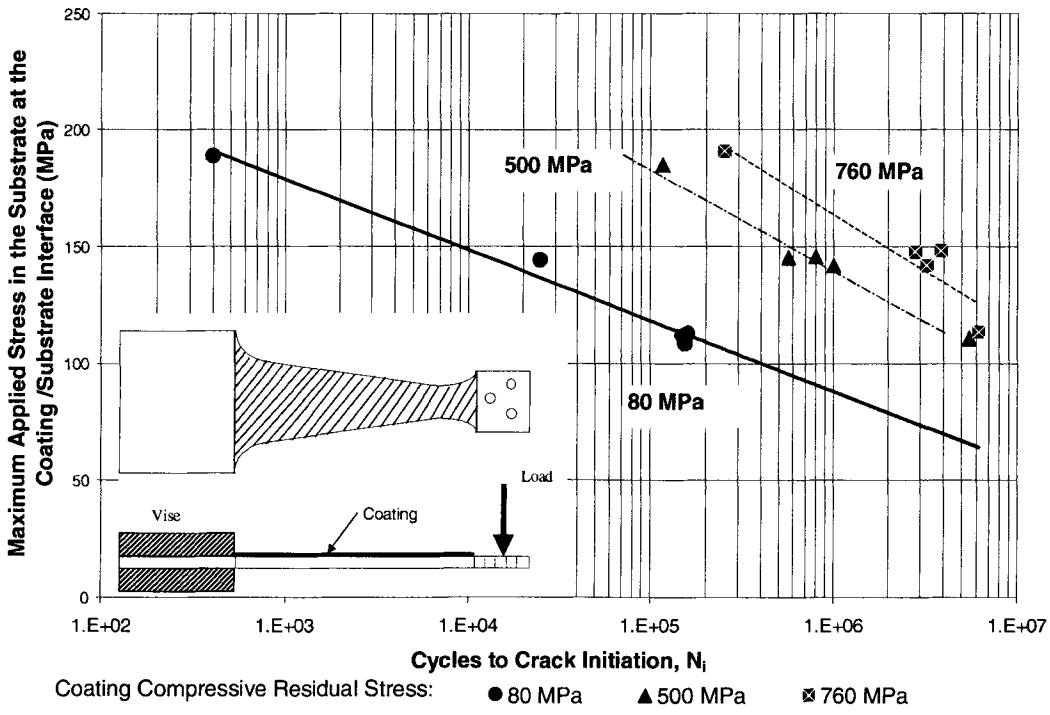

Fig. 7 *S-N* curve for cycles to crack initiation, constant deflection, HVOF-tungsten carbide on 6061-T6511

500 MPa failed at 9×10^5 cycles and specimens with a compressive residual stress of 760 MPa failed at 3.4×10^6 cycles. In the example case (145 MPa maximum applied stress in the substrate at the interface), a specimen with an average coating compressive residual stress of 500 MPa was found to have ten times longer life than a specimen with a coating compressive residual stress of 80 MPa. A specimen with an average coating compressive residual stress of 760 MPa was found to have 35 times longer life than a specimen with an average coating compressive residual stress of 80 MPa at 145 MPa applied stress.

The curve for the Al base material is shown for comparison. Notice that the fatigue life curve for the specimens with 760 MPa compressive residual stress approaches the curve for the bare aluminum specimens.

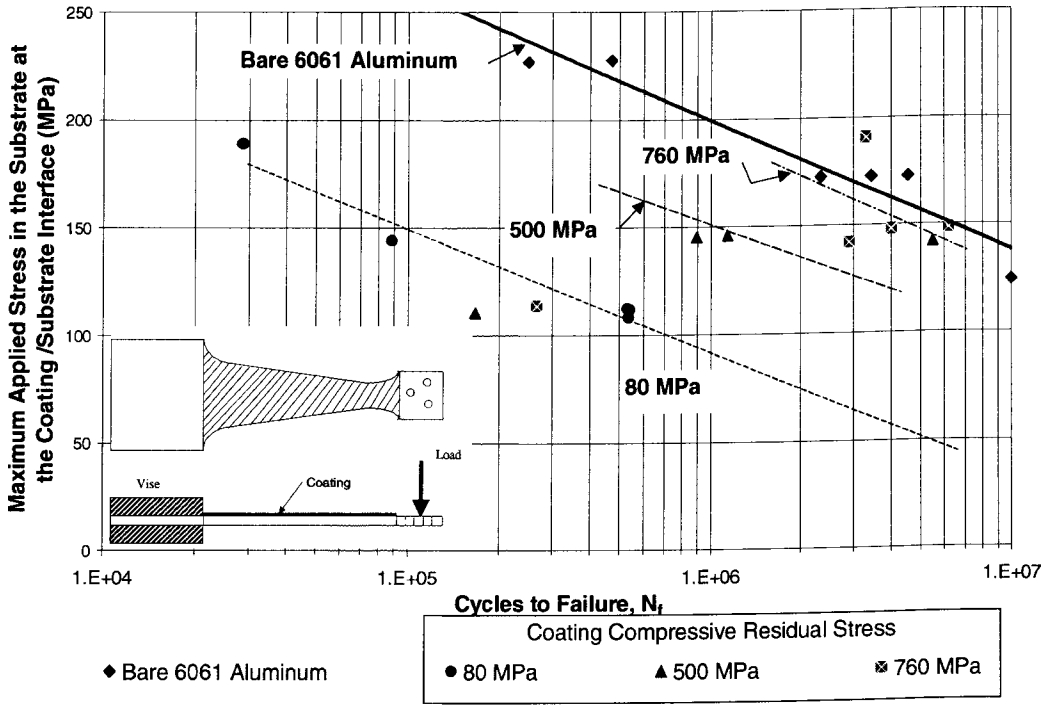

Fig. 8 *S-N* curve for cycles to complete failure, constant deflection, HVOF-tungsten carbide on 6061-T6511

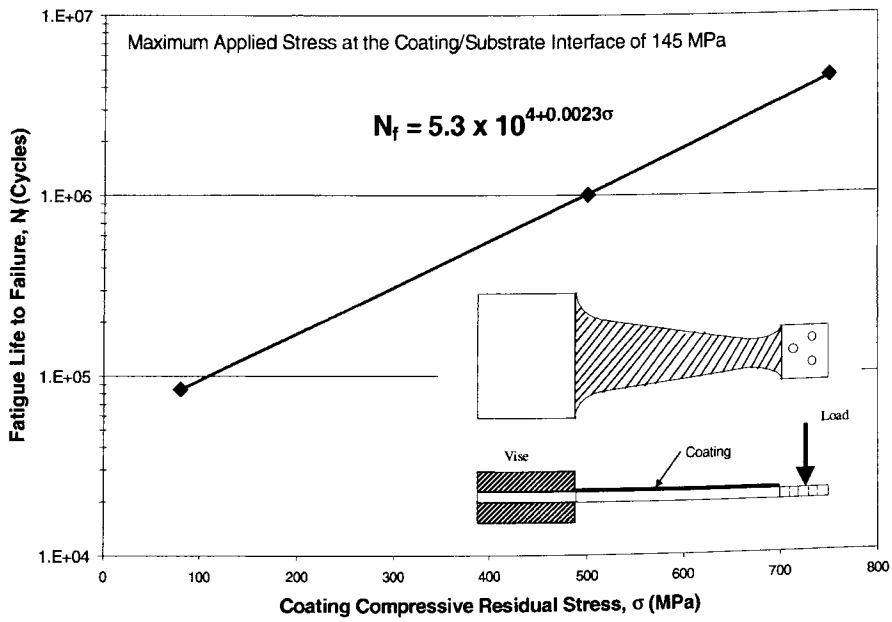

Fig. 9 Trend of average compressive residual stress in the coating to fatigue life at 145 MPa (21 ksi) maximum applied stress in the substrate at the coating substrate interface

5.5 *Trend of Average Coating Residual Stress Level and Fatigue Life*

At the applied bending stress levels used in this testing, the increase in coating life can be correlated with the compressive residual stress in the coating. Shown in Fig. 9 is a semi-log graph of cycles to failure versus average coating compressive residual stress at a maximum applied stress of 145 MPa. At this maximum applied stress, the fatigue life of the coated part with a neutral compressive stress in the coating is 85,000 cycles to failure. When the compressive residual stress in the coating is increased to 760 MPa, the number of cycles to failure increased to 4.5 million cycles.

However, at another maximum applied stress, the increase in the number of cycles can be significantly different. This increase in the number of cycles to failure is very dependent on the maximum applied stress.

6. Summary and Conclusions

The objective of determining the effect of average coating residual stress on fatigue crack initiation and fatigue failure was accomplished for constant deflection bend testing. The increase in fatigue life of the specimens with higher average coating compressive residual stress is clearly demonstrated by the results of these tests, where the loading is cantilever beam bending. However, modes of failure other than fatigue failures (for example, spalling) occur in these components. It should be noted that increasing the compressive residual stress in the coating beyond some value that remains to be determined in each intended application might significantly increase the likelihood of failure due to spalling.

An important step toward reaching the goal of the larger program has been taken. That goal is to utilize WC thermal spray coatings in applications where surfacing is currently being done by anodizing. The results of this work provide a better understanding of how to improve the fatigue behavior of WC coatings for bending fatigue conditions. Attention to the residual stress in the coating and the process parameters that create those residual stresses is necessary. Knowledge of the residual stress level in the coating combined with a known maximum applied stress can be used to estimate the fatigue life of parts subjected to cyclic bending with constant maximum deflection.

Acknowledgments

The authors acknowledge the Oklahoma Center for the Advancement of Science and Technology (OCAST), Southwest Aeroservice, Inc., and The University of Tulsa for support of this work.

References

1. J.M. Quets, "High Cycle Fatigue Properties of Chrome Plated 7075-T73 Aluminum and 4340 Steel," Union Carbide, Technical Note No. 91-03, 1991
2. R.W. Landgraf and R.A. Chernenkoff, Residual Stress Effects on Fatigue of Surface Processed Steels, *Analytical and Experimental Methods for Residual Stress Effects in Fatigue,* STP 1004, ASTM, 1988, p 1-12
3. S.K. Koh and R.I. Stephens, Mean Stress Effects on Low Cycle Fatigue for a High Strength Steel, *Fatigue Fract. Eng. Mater. Struct.,* Vol 14 (No. 4), 1991, p 413-428
4. D.J. Greving, E.F. Rybicki, and J.R. Shadley, Through-Thickness Residual Stress Evaluations for Several Industrial Thermal Spray Coatings Using a Modified Layer-Removal Method, *J. Therm. Spray Technol.,* Vol 3 (No. 4), 1994, p 379-388
5. E.F. Rybicki, J.R. Shadley, Y. Xiong, and D.J. Greving, A Cantilever Beam Method for Evaluating Young's Modulus and Poisson's Ratio of Thermal Spray Coatings, *J. Therm. Spray Technol.,* Vol 4 (No. 4), 1995, p 377-383
6. Y. Xiong, "A Cantilever Beam Method for Evaluating Young's Modulus and Poisson's Ratio of Thermal Spray Coatings," Master of Science thesis, The University of Tulsa, 1994
7. R.T.R. McGrann, J.R. Shadley, E.F. Rybicki, B.E. Bodger, and W.A. Emery, Thermal Spray Coatings for Aircraft Landing Gear Components, *Proc. of the AESF 1998 Aerospace/Airline Plating Forum,* p 39-46
8. D.J. Greving, "Residual Stress and Thermal Spray Coating Performance," Ph.D. dissertation, The University of Tulsa, 1995
9. ASM, Vol 1, *Metals Handbook,* 8th ed., American Society for Metals, 1961, p 946
10. F.P. Beer and E.R. Johnston, Jr., *Mechanics of Materials,* 2nd ed., p 204-207